UTILIZATION OF HYPERSPECTRAL IMAGING FOR CLASSIFYING POTATO TUBERS BASED ON ANTHOCYANIN CONTENT

Elmasry, G.[1]; S. M. Radwan[1] and N. Wang[2]
[1] Agricultural Engineering Department, Faculty of Agriculture, Suez Canal University, Ismailia, Egypt.
[2] Department of Bioresource Engineering, McGill University, Macdonald Campus. 21,111 Lakeshore Road, Ste-Anne-de-Bellevue, Quebec. Canada. H9X 3V9.

ABSTARCT

Hyperspectral imaging technique in visible and near infrared (VIS/NIR) region with the range of 400 to 1000 nm was established for non-destructive assessment of anthocyanin concentration in three potato cultivars (Russet Burbank, Norland and Yokon Gold). Sixty tubers (20 tubers from each cultivar) were imaged with the hyperspectral imaging system and the anthocyanin concentrations were measured in the laboratory. Simple linear regression models were built between the anthocyanin concentration in the tested samples and their spectral responses at 550 nm. The prediction model performed well and predicted the anthocyanin content with standard error of calibration (SEC) equal to 7.22 in the calibration set (45 tubers) and correlation coefficient of 0.91. In the validation set (15 tubers), the model also achieved high success for predicting anthocyanin concentration with SEP of 11.95 and correlation coefficient of 0.91.
Keywords: Hyperspectral imaging, potato, anthocyanin, discriminant analysis.

INTRODUCTION

Egypt is considered one of the most important producers of fruits and vegetables in Africa and Middle East region. The Egyptian production from fruits and vegetables is 24.1 million tons which represents 1.74 % of the overall world production (FAO, 2004). Therefore, governmental agencies and industries have committed cooperative efforts to improve the overall quality and safety of food to gain a share in the international markets.

In general, quality of produced encompasses sensory attributes, nutritive values, chemical constituents, mechanical properties, functional properties and presence of defects. Instruments can approximate human judgments by imitating the way people test the product or by measuring fundamental properties and combining those mathematically to categorize the quality. Only people can judge quality, but instruments that measure quality-related attributes are vital for research and for inspection (Abbott, 1999). Food technologists as well as agricultural engineers are interested in quality properties of food materials in order to determine how food or fruits will be handled during processing, to get an indication of the products' quality, and to understand why consumers prefer certain food or fruits. Moreover, the trend towards continuous automated production in place of human assisted operation necessitates the measurement of fruit and vegetable properties, particularly in the area related to on-line or rapid process control applications (Abdullah et al., 2004). Combined with an illumination system, a computer

vision system is typically based on a personal computer in connection with electrical and mechanical devices to replace human manipulative effort in the performance of a given process (Du ad Sun, 2006). Image processing and image analysis are the core of computer vision, involving mathematics, computer science and software programming.

As an extension for computer vision, spectral imaging has been invented to integrate spectroscopic and spatial (imaging) information. Spectral imaging involves measuring the intensity of diffusely reflected light from a surface at one or more wavelengths with relatively narrow band-paths. Spectral imaging goes beyond conventional imaging and spectroscopy to acquire both spectral and spatial information from an object simultaneously. Since image data are considered two dimensional, by adding a new dimension of "spectrum" information, the spectral image data can be perceived as a three-dimensional data cube (Chao et al., 2001).

A major challenge facing the food industry is to increase efficiency of production and at the same time maintain or improve product quality. Consequently, rapid techniques are increasingly required in production lines for quality control, and for optimized utilization of variation in raw materials. The industrial demands for such methods are growing, and current needs span a broad range of applications, such as determination of chemical composition in various food, effective measurement of rancidity, detection of foreign substances or bodies, and monitoring of complex reactions. Therefore, development of nondestructive technology for internal attributes will help the industry to provide better fruit for the consumer and, thus, improve industry competitiveness and profitability (Park et al., 2003; Lu, 2004; Peng and Lu, 2004; Peng and Lu, 2005). Thus, nondestructive sensing methods of internal quality would allow the fruit industry to deliver better quality, more consistent fruit to the consumer (Berardoa et al., 2004).

Generally, color is the basis for sorting many products into commercial grades, but concentration of pigments or other specific constituents might provide a better quality index. Color relates more directly to consumer perception of appearance, pigment concentration may be more directly related to maturity, and concentration of certain other constituents relates more closely to flavour. Anthocyanin is one of the six subgroups of the large and widespread group of plant constituents known as flavonoids which is nutritionally important. Anthocyanin is of nutritional interest because of their marked daily intake and its reported positive effects in the treatment of various diseases.

This study intended to establish a hyperspectral imaging system accompanied with image processing algorithms to assess anthocyanin concentration in potato non-destructively.

MATERIALS AND METHODS

The experimental work of this study was carried out in an Instrumentation and Sensing Laboratory, Bioresources Engineering Department, Faculty of Agricultural and Environmental Sciences, McGill

University, Canada. The main purpose of this study was to establish a hyperspectral imaging system accompanied with image processing algorithms to assess anthocyanin concentration in three cultivars of potato non-destructively.

Potato sample sets

Three cultivars of potato (Russet Burbank, Yokon Gold, and Norland) containing different concentration of anthocyanin were purchased from local retail stores. The Norland cultivar has a red peel and it is expected to contain abundant level of anthocyanin content. On the other hand, the Russet Burbank cultivar has a white peel, so that its anthocyanin content is rather small. The Yokon cultivar has yellow to brown peel, so that it contains intermediate level of anthocyanin. By choosing these three different cultivars, wide variation in anthocyanin content is vital for developing prediction models. Good appearance of the tested tubers is essential for the experiment. All abnormal tubers were discarded. Twenty tubers from each cultivar free from any abnormal features such as defects, bruises, diseases, and contaminations were selected. The tested tubers were randomly divided into two major divisions. The first division consisted of 45 tubers was used as a calibration/training set. The second division consisted of 15 tubers was used for model validation and to verify the prediction power of the calibration model.

Hyperspectral imaging system

A laboratory hyperspectral imaging system was constructed as shown in Fig. (1). It is composed of the following five components: (1) CCD camera (PCO-1600, Pco. Imaging, Germany), (2) spectrograph (ImSpector V10E, Optikon Co., Canada) coupled with a standard C-mount zoom lens, (3) illumination unit consisting of two 50W halogen lamps adjusted at angle of 45° to illuminate the camera's field of view, (4) fruit holder surrounded by a cube tent made from white nylon to diffuse the light and provide a uniform lighting condition, and (5) laptop computer.

The assembly disperses the incoming light into the spectral and spatial matrices and then projects them onto the CCD. The optics, spectrograph and the camera, has high sensitivity in the spectral range from 400 to 1000 nm and the exposure time was adjusted at 200 ms throughout the whole test. The distance from lens to the fruit surface was fixed at 40 cm. The camera-spectrograph assembly is provided with a stepper motor to move this unit through the camera's field of view to scan the fruit line-by-line.
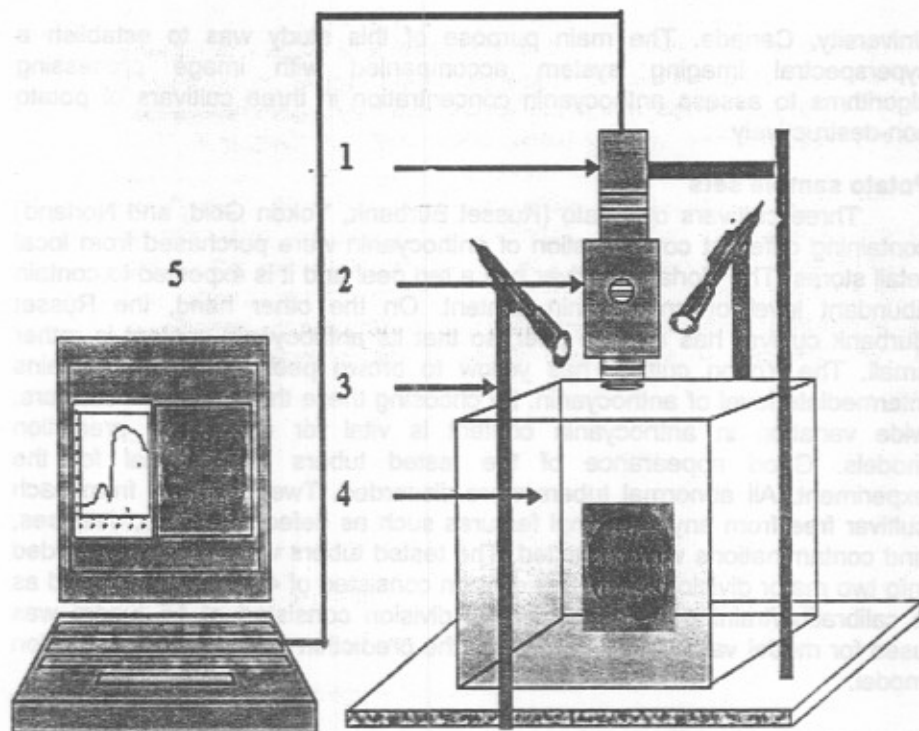
Fig. (1): Detailed components of the hyperspectral imaging system
(1) CCD camera, (2) Spectrograph with a standard C-mount zoom lens, (3) Halogen lighting unit, (4) White nylon fabric tent, and (5) Computer supported with image acquisition software.

After finishing the scans on the entire fruit, the spatial-by-spectral matrices were combined to construct a three-dimensional (x, y, λ) spatial and spectral data space. Images were binned during acquisition in spatial direction to provide images with spatial dimension (x,y) of 400×400 pixels with 826 spectral bands (λ) from 400 to 1000 nm. The hyperspectral imaging system was controlled by the computer which is supported with Hypervisual Imaging Analyzer (ProVision Technologies, Stennis Space Center, USA) for spectral image acquisition, binning, and camera and motor control.

Calibration of the hyperspectral images

All the acquired hyperspectral images were processed and analyzed using Environment for Visualizing Images (ENVI 4.2) software (Research Systems Inc., Boulder Co., USA). Standard white and a dark reference were acquired for calibrating the hyperspectral images. The dark reference was used to remove the effect of dark current of the CCD detectors. These reference spectra were used to convert the raw reflectance for each pixel in a tuber into relative reflectance using the equation (1). The calibrated image (R)

is then calculated using equation (1) as described by Mehl *et al.* (2002) and Xing and De Baerdemaeker (2005) as follow:

$$R = \frac{R_o - D}{W - D} \times 100 \qquad (1)$$

Where (R_o) is the recorded hyperspectral image, (D) is the dark image (with 0% reflectance) recorded by turning off the lighting source with the lens of the camera completely closed and (W) is the white reference image (Teflon white board with 99% reflectance). The resulting corrected images were used to extract information about the spectral properties of the whole tuber surface.

Collecting spectral signature of each tuber

Due to variation in anthocyanin content among tested tubers, each tuber reflects, absorbs, and emits electromagnetic energy in distinctive patterns especially at the sensitive wavelength of anthocyanin. In essence, anthocyanin shows characteristic maxima of absorption, one in the ultraviolet region (approximately at 240 nm) and two in the visible region (approximately 415 and 550 nm). The wavelengths of these absorbance peaks can differ slightly by a few nanometers among various anthocyanins. In this study, the absorbent band of anthocyanin is located around 550 nm which uniquely characterize and identifies the tuber in terms of their anthocyanin content. So, the lower reflectance (high absorbance) of such tuber at this wavelength indicates higher anthocyanin concentration in this tuber. To collect the spectral response of each tuber, a binary mask was first created to produce an image containing only the tuber in the middle of the image, avoiding any interference from the background. Image at 500-nm band was picked up for this task because the tuber appeared opaque compared with the background and can be segmented easily by simple thresholding. All active pixels in the segmented image were used as a mask and act as an area of interest (AOI). At each pixel of AOI, the relative reflectance was recorded at each wavelength from 400 to 1000 nm. Then, an average reflectance spectrum was determined by averaging the relative reflectance spectra of all pixels in the AOI. In total, 60 average spectra (400-1000 nm) representing all tested 60 tubers were recorded and stored in the computer for calibration model development. A clear picture of this step is depicted in Fig. (2).
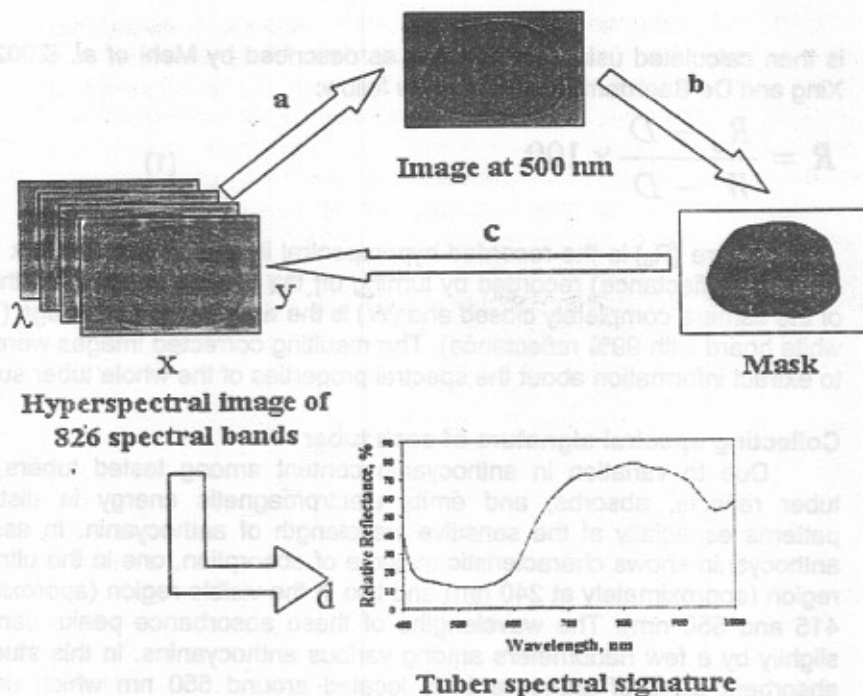
Image at 500 nm

Hyperspectral image of
826 spectral bands

Mask

Tuber spectral signature

Fig. (2): Extraction of the tuber spectral signature.
a) Selecting 500 nm image, b) Binarization (defining AOI, area of
interest), c) Applying the mask, and d) Calculating tuber spectral
signature using those only at the black pixels in the mask (AOI).

Measurement of anthocyanin concentration

After acquiring spectral images, each tuber was peeled with approximately 0.5 cm thickness for total anthocyanin content determination following the method reported by Miyanaga et al. (2000). Exactly 0.5 gm was grinded with 2 ml of extraction solution (15:85 ml 0.1% HCl : Methanol) using an electrical tissue chopper (Biospec Products Inc. Model 398, Dremel Racine WI, USA) for 30 sec at 10000 rpm, then samples were vortexed (Vortex-2 Gene, Scientific Industries Inc, Biochemia, NY, USA) for 5 sec and kept overnight in the fridge. Samples were centrifuged at 4000 rpm for 10 min (HN-S Centrifuge, International Equipment Co., Needham Heights, USA). 10 μL were taken from the extract and diluted 1 : 4 with the extraction solution for colour measurements at 530 nm by ELISA plate reader (BIO-TEK Synergy HT, Vermont USA). Extraction solution was used as a blank. Total anthocyanin content was measured as mg/gm fresh weight.

Building prediction model

To develop a simple regression model to relate the spectral feature of the tested tubers with anthocyanin concentration. The wavelength at 550 nm was chosen to build such a model because the difference in anthocyanin content in the tubers can be detected at this band. Once the linear regression model was determined, its equation was used to predict the anthocyanin

concentration of tubers in the calibration and validation sets. Actual values of the anthocyanin concentration were plotted to visually evaluate the performance of the model. Only 45 tubers (training set) were used to make this relationship and to extract the simple regression model for further anthocyanin prediction. Later, this regression model was validated with other group containing 15 tubers (validation set). The validity of the regression model was evaluated by the standard error of calibration (SEC), standard error of prediction (SEP) and the correlation coefficient (r) between the predicted and measured values of the anthocyanin concentration. A good model should have a low SEC, a low SEP, a high correlation coefficient, and a small difference between SEC and SEP. These criteria were calculated according to the formulas 2, 3, and 4 defined by Lammertyn et al (1998); Gómez et al (2006) and Nagata et al (2005):

$$SEC = \sqrt{\frac{1}{I_C - 1} \sum_{i=1}^{I_C} (\hat{y}_i - y_i)^2} \qquad (2)$$

$$SEP = \sqrt{\frac{1}{I_p - 1} \sum_{i=1}^{I_p} (\hat{y}_i - y_i - bias)^2} \qquad (3)$$

$$bias = \frac{1}{I_p} \sum_{i=1}^{I_p} (\hat{y}_i - y_i) \qquad (4)$$

Where

$\hat{y}_i$: Predicted value of an attribute in fruit number i,

y_i : Measured value of an attribute in fruit number i,

I_c : Number of tubers (spectra) in the calibration set (45),

I_p : Number of tubers (spectra) in the validation set (15).

Bias: Average difference between predicted and actual values.

RESULTS AND DISCUSSIONS

Characteristics of Potato Reflectance Spectra

The laboratory measurements of average anthocyanin concentrations in the tested cultivars were 7.92, 33.63, 50.47 ppm for Russet Burbank, Yokon Gold and Norland, respectively. On the other hand, Fig. (3) shows 60 reflectance spectra in the range from 400 to 1000 nm of potato collected from the three cultivars (20 spectra for each cultivar). In spite of anthocyanin concentration in the tested samples, the reflectance curves of potato were rather smooth across the entire spectral region. In all samples, the reflectance curves had two major absorption regions around 550 and 960 nm.

Elmasry, G. et al.

J. Agric. Sci. Mansoura Univ., 32 (5), May, 2007

The regions at 550 represent anthocyanin pigments which gave the red colour of the tuber (Abbott *et al.*, 1997 and Seeram *et al.*, 2006). Meanwhile, the region at 960 nm was due to water absorption (Keskin *et al.*, 2004).

The only change among spectra due to the difference in anthocyanin content was observed in the visible bands between 500 to 600 nm. Based on the reflectance plots of the samples with varying anthocyanin contents, the band centered at 550 nm can be selected as a significant wavelength. The samples that had higher amount of anthocyanin had lower reflectance values around 550-nm band. Therefore, Norland cultivar had the highest anthocyanin content. Also, the reflectance from both Russet Burbank and Yokon Gold cultivars was consistently lower than that of Russet Burbank cultivar indicating that the Russet Burbank and Yokon Burbank cultivars had lower anthocyanin content. It was obvious that the trend of anthocyanin of the tested cultivars obtained from the spectral curves at 550-nm band is corresponding to the same trend resulting from the laboratory measurement. The arrow shown in Fig. (3) indicates the direction of increasing anthocyanin concentration.
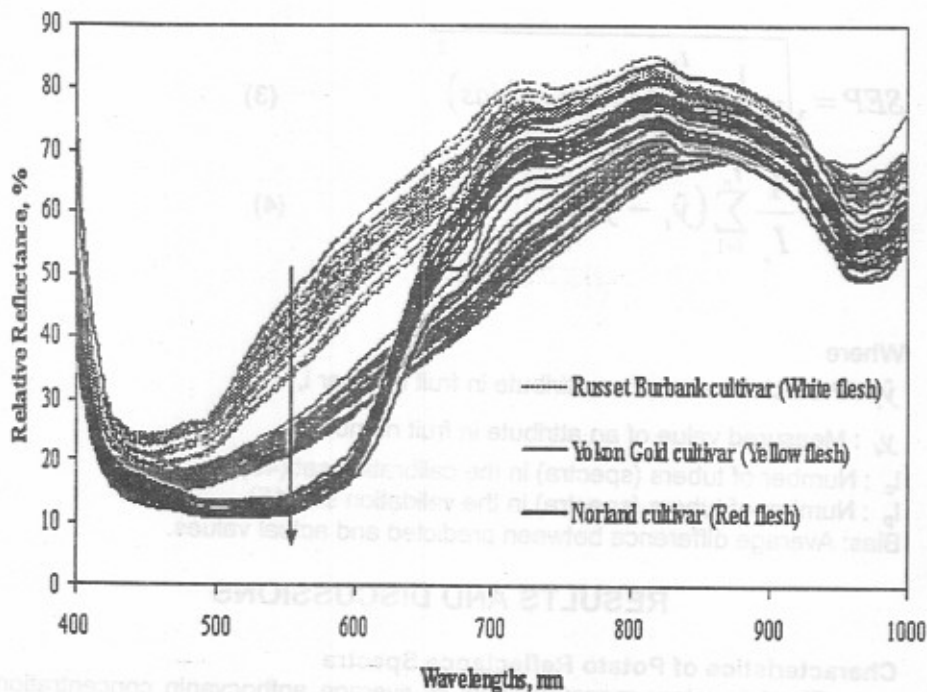

Fig. (3): Typical reflectance of VIS/NIR spectra of potato cultivars of different peel colours.

Prediction by linear regression

The significant wavelength at 550 nm was used to build a linear regression model between the reflectance at this wavelength and the

measured values of anthocyanin in the calibration set consisting of 45 tubers. Figure (4) compares the actual and predicted anthocyanin contents using the regression model with only the reflectance at 550-nm band.

It is clear that, the model performed well and predicted the anthocyanin content with SEC values of 7.22 in the calibration set and correlation coefficient of 0.91. The calculated regression model produced high performance not only in the training/calibration set but also in the validation set. In the validation set the model also achieved high success for predicting anthocyanin concentration in the other 15 tubers with SEP of 11.95 and correlation coefficient of 0.91. Nevertheless, the confidence intervals at significant level of 95 % which are plotted as dashed lines in Fig. (4) contained most of the predicted data points. This suggests that the regression model with a single wavelength variable centered at 550 nm had a good performance for predicting anthocyanin concentration.
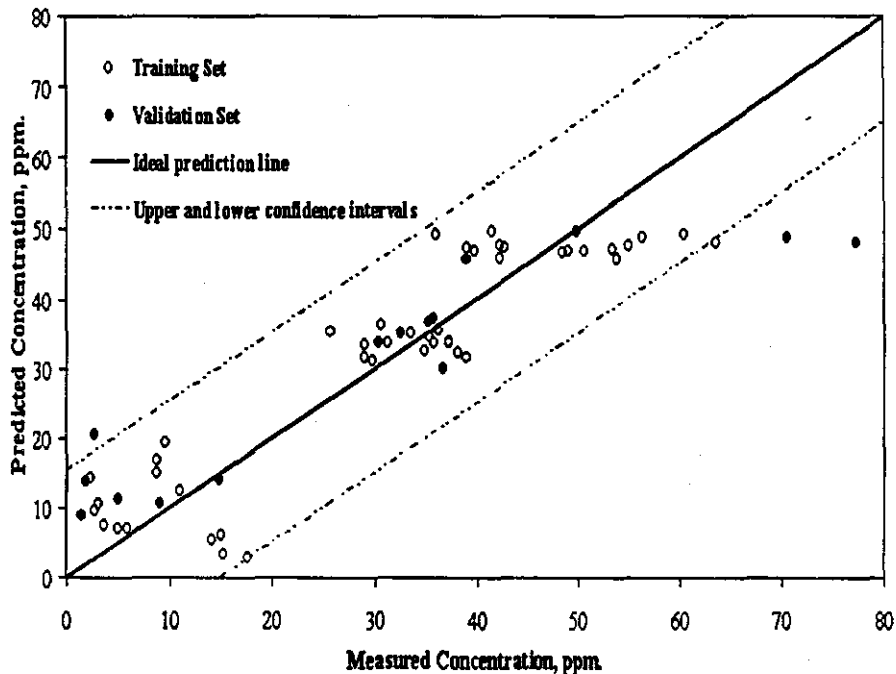

Fig. (4): Measured and predicted anthocyanin concentration using the reflectance at 550-nm band.

Moreover, to recognize the discriminatory power of the 550-nm band for distinguishing the anthocyanin level in the tested samples, discriminant analysis was conducted using the reflectance at 550 nm as a discriminating variable. The potato samples were first classified according to their anthocyanin concentration level to three groups (low, medium and high). Then, the discriminant analysis test was carried out to know the capability of the discriminating variable (550-nm band) for classifying the same sample to its initial groups. As shown in Fig. (5), the variance among predefined groups

was maintained in the first two factors (F1 = 77.32% and F2 = 22.68%) which represent the total variance among the potato groups. The plot clearly indicated that the discriminating variable (550-nm band) had a great power for classifying potato samples according to their anthocyanin level without any interference among groups. The overall conclusion is that the 550-nm band had a great power not only for predicting anthocyanin concentration with good precision but also for classifying the potato according to its anthocyanin content with high accuracy.
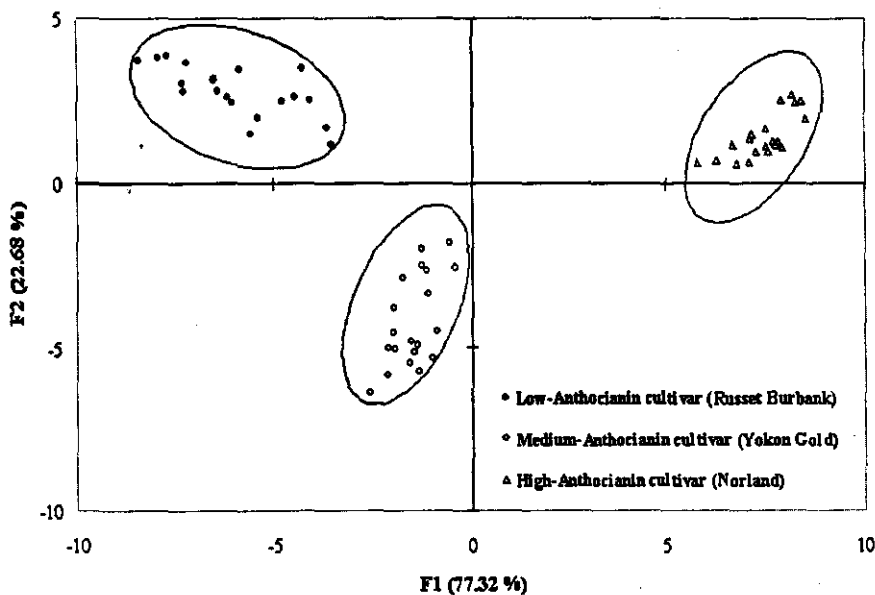

Fig. (5): Discrimination analysis for classifying potato samples depending on their anthocyanin content using the reflectance at 550 nm band.

CONCLUSION

Non-destructive assessment of anthocyanin concentration in three potato cultivars (Russet Burbank, Norland and Yokon Gold) was carried out by a hyperspectral imaging system in visible and near infrared (VIS/NIR) region with the range of 400 to 1000 nm. Simple linear regression models were built between the anthocyanin concentration in the tested samples and their spectral responses at 550-nm band. The results revealed that the regression model with a single wavelength variable centered at 550-nm band had a good performance for predicting anthocyanin concentration. This could be ascribed to the absorption characteristics of anthocyanin at this wavelength. For the calibration set, the standard error of calibration (SEC) and correlation coefficient were of 7.22 and 0.91 respectively. In the validation set, the model also achieved high success for predicting anthocyanin concentration with SEP of 11.95 and correlation coefficient of

0.91. The optimistic results achieved from this study promoted more and more investigations in this field for measuring other quality attributes in different fruits and vegetables

ACKNOWLEDGMENT

REFERENCES

Abbott, J.A. 1999. Quality measurement of fruits and vegetables. Postharvest Biology and Technology 15 (3): 207-225.

Abbott, J.A.; Lu, R.; Upchurch, B.L. and Stroshine, R.L. 1997. Technologies for non-destructive quality evaluation of fruits and vegetables. Hortic. Rev.20:1-120.

Abdullah, M.Z.; Guan, L.C.; Lim, K.C. and Karim, A.A. 2004. The applications of computer vision system and tomographic radar imaging for assessing physical properties of food. Journal of Food Engineering 61 (2): 125-135.

Berardoa, N.; Brennab, O.V.; Amatoa, A.; Valotia, P.; Pisacanea, V. and Motto, M. 2004. Carotenoids concentration among maize genotypes measured by near infrared reflectance spectroscopy (NIRS). Innovative Food Science and Emerging Technologies 5: 393– 398.

Chao, K.; Chen, Y.–R.; Hruschka, W.R. and Park, B. 2001. Chicken heart disease characterization by multi-spectral imaging. Applied Engineering in Agriculture 17(1): 99-106.

Du, C.-J. and Sun, D.-W. 2006. Learning techniques used in computer vision for food quality evaluation: A review. Journal of Food Engineering 72 (1): 39-55.

FAO. (2004). Food and Agriculture Organization Statistics, FAOSTAT. www.fao.org

Gómez, A.H.; He, Y. and Pereira, A.G. 2006. Non-destructive measurement of acidity, soluble solids and firmness of Satsuma mandarin using VIS/NIR-spectroscopy techniques. Journal of Food Engineering 77(2): 3313-319.

Keskin, M.; Dodd, R.B.; Han, Y.J. and Khalilian, A. 2004. Assessing nitrogen content of golf course turfgrass clippings using spectral reflectance. Applied Engineering in Agriculture 20(6): 851-860.

Lammertyn, J.; Nicolaï, B.; Ooms, K.; De Smedt, V. and De Baerdemaeker, J. 1998. Non-destructive measurement of acidity, soluble solids, and firmness of Jonagold apples using NIR spectroscopy. Transactions of the ASAE 41(4): 1089-1094.

Lu, R. 2004. Multispectral imaging for predicting firmness and soluble solids content of apple fruit. Postharvest Biology and Technology 31 (2): 147-157.

Mehl, P.M.; Chao, K.; Kim, M. and Chen, Y.R. 2002. Detection of defects on selected apple varieties using hyperspectral and multispectral image analysis. Applied Engineering in Agriculture 18(2): 219-226.

Miyanaga, K.; Seki, M. and Furusaki, S. 2000. Quantitative determination of cultured strawberry-cell heterogeneity by image analysis: effects of medium modification on anthocyanin accumulation. Biochemical Engineering Journal 5: 201–207.

Nagata, M.; Tallada, J.G.; Kobayashi, T. and Toyoda, H. 2005. NIR Hyperspectral Imaging for Measurement of Internal Quality in Strawberries. ASAE Annual International Meeting, Paper No. 053131, Tampa, Florida, USA.

Park, B.; Abbott, J.A.; Lee, K.-J.; Choi, C.-H. and Choi, K.-H. 2003. Near-Infrared diffuse reflectance for quantitative and qualitative measurement of soluble solids and firmness of Delicious and Gala apples. Transactions of the ASAE 46(6): 1721-1731.

Peng, Y. and Lu, R. 2004. Predicting apple fruit firmness by multispectral scattering profiles. ASAE/CSAE Annual International Meeting, Paper No. 046117, Ottawa, Ontario, Canada, 1-4 August 2004.

Peng, Y. and Lu, R. 2005. Modeling multispectral scattering profiles for prediction of apple fruit firmness. Transactions of the ASAE 48(1): 235–242.

Seeram, N.P.; Lee, R., Scheuller, H.S. and Heber, D., 2006. Identification of phenolic compounds in strawberries by liquid chromatography electrospray ionization mass spectroscopy. Food Chemistry 97 (1): 1–11.

Xing, J. and De Baerdemaeker, J. 2005. Bruise detection on 'Jonagold' apples using hyperspectral imaging. Postharvest Biology and Technology 37 (1) 152-162.

استخدام التصوير الطيفى لتصنيف درنات البطاطس تبعاً لمحتواها من الأنثوسيانين
جمال المصرى¹، شريف محمد عبد الحق رضوان¹ و نينج وانج²
¹ قسم الهندسة الزراعية – كلية الزراعة – جامعة قناة السويس– الإسماعيلية
² قسم هندسة المصادر الحيوية – جامعة ماكجيل – كندا

إن المنتج الغذائى ذو الجودة العالية لابد أن يكون خالياً من العيوب والأمراض والكدمات وأن يكون ذو قيمة غذائية عالية فضلا عن الشكل واللون والمذاق المميز لهذا المنتج. ويمكن للعامل المدرب ذو الخبرة العالية تحديد الصفات والخصائص الظاهرية للمنتج بمجرد النظر أثناء عمليات الفرز والتدريج. ولكن تبقى المشكلة قائمة لتحديد صفات الجودة الداخلية للمنتج من حيث محتواه على عناصر غذائية أو مكونات كيماوية بعينها مما يستلزم أخذ عينات من المنتج لاختبارها معملياً والحكم على باقى المنتج تبعاً لنتيجة هذه العينة. وبالرغم من تطبيق هذه الطريقة فى معظم وحدات الإنتاج الا أنه يعيبها أنها طريقة مكلفة وبطيئة وتتطلب تحطيم العينة نفسها لإجراء هذه الاختبارات عليها. ولهذا كان الغرض من هذه الدراسة هو تطوير وحدة تصوير طيفى فـى المـدى المرئـى والقريب من الأشعة تحت حمراء (VIS/NIR) فى المدى ٤٠٠–١٠٠٠ نانومتر لتقدير صـبغة الأنثوسيانين فى ثلاثة أصناف مـن البطـاطس هـى Russet Burbank, Norland and Yokon Gold كطريقة غير محطمة للدرنات. وقد تم أخذ ٦٠ درنة (٢٠ درنة من كل صنف) وتقسيمها الى مجموعتين: مجموعة اختبارية وتتكون من ٤٥ درنة وتستخدم فى استخراج نمـوذج للتنبؤ بمحتوى الانثوسيانين، ومجموعة تأكيدية وتتألف من ١٥ درنة للتأكد من كفاءة نموذج التنبؤ. وقد تم أخذ الصور الطيفية للدرنات بحيث تتألف كل صورة من ٨٢٦ طول موجى يختلف شـكل للدرنة فيها عند كل طول موجى تبعا للصفات الكيماوية لهذه الدرنات. بعدها تم أخذ الدرنات وتقدير محتواها من الانثوسيانين معملياً وذلك لربط النتائج المتحصل عليها من الصور الطيفيـة ومثيلتهـا المقدرة معملياً.

كان الإختلاف الواضح فى الإستجابات الطيفية للأصناف الثلاثة محصورا فى المجال المرئى فـى المدى ٥٠٠–٦٠٠ نانومتر وأن الطول الموجى عند ٥٥٠ نانومتر يمكن إستخدامه لتوضيح الفروق بين الأصناف الثلاثة من حيث محتواها من صبغة الأنثوسيانين.

ولذلك فقد تم عمل نموذج تنبؤ بين الانعكاس الضوئى للدرنات عند الطول الموجى ٥٥٠ نانومتر وبين محتوى الدرنات من صبغة الأنثوسيانين. وقد أعطى نموذج التنبؤ عند الطول الموجى ٥٥٠ نانومتر أداءً جيداً للتنبؤ بتركيز الأنثوسيانين فى الثلاثة أصناف تحت الدراسة بمعامل ارتباط ٠,٩١ وبقيمة خطأ SEC تعادل ٧,٢٢ فى حالة المجموعة الإختبارية، وبمعامـل ارتبـاط ٠,٩١ وقيمة خطأ SEP تعادل ١١,٩٥ للمجموعة التأكيدية.

ولهذا تم استنتاج أن الطول الموجى ٥٥٠ نانومتر له كفاءة عالية ليس فقط للتنبؤ بتركيز الأنثوسيانين فى درنات البطاطس ولكن أيضاً لتقسيم تلك الدرنات تبعـاً لمحتواهـا مـن صـبغة الأنثوسيانين بدقة عالية.